Long-term treatment with salicylate enables NMDA receptors and impairs AMPA receptors in C57BL/6J mice inner hair cell ribbon synapse

WANMING CUI[*], HAOLIN WANG[*], YU CHENG, XIAORUI MA, YU LEI, XINGXING RUAN, LIN SHI and MEI LV

Department of Otorhinolaryngology, The First Affiliated Hospital of Dalian Medical University,
Dalian, Liaoning 116013, P.R. China

Abstract. Salicylate is widely used to produce animal models of tinnitus in mice and/or rats. The side effects on auditory function, including hearing loss and tinnitus, are considered the results of the auditory nerve dysfunction. A recent study indicated that chronic treatment with salicylate for several weeks reduces compressed action potential amplitude, which is contradictory to the studies reporting excessive activation of N-methyl-D-aspartate receptors (NMDAR) in tinnitus-induced animals. The specific aims of the experiment were to detect the effect of salicylate on the inner hair cells (IHCs), ribbon synapse, as well as the association between the hearing threshold and the number of mismatched ribbon synapses. In the present study, mice were injected intraperitoneally with a low dose of salicylate (200 mg/kg) for 14 days. The auditory brainstem response and otoacoustic emission were measured to assess auditory function of the mice. The postsynaptic regions of IHC were identified with two types of immunostaining targets: Postsynaptic density protein 95 and Glu2/3. The number of spheres was counted and the synapses were reconstructed in 3-dimensional images. Increases in distortion product otoacoustic emissions amplitudes of the salicylate group were detected, however, an elevation in the hearing threshold was also observed. A mismatch between pre-and post-ribbon synapses was observed. In addition, the cochlear components, including the numbers of outer hair cells and IHCs, were unlikely to be affected by salicylate. IHC ribbon synapses were more susceptible to salicylate stimuli. Furthermore, mismatch of pre- and post-ribbon synapses may indicate a competitive inhibition between NMDAR and α-amino-3-hydroxy-5-methyl-4-isoxa-zole-propionate receptors and dysfunction of ribbon synapses.

Introduction

Subjective tinnitus is characterized by the perception of a sound in the absence of an acoustic source in the environment. It is a nerve disorder which is accompanied with hearing loss, cochlear damage (1) and stress (2-6). Due to demographic changes and to the increasing use of personal headsets, notably by young people (7), tinnitus is becoming a cumulative challenge. It is estimated that ~50 million adults have experienced tinnitus, whereas 16 million are currently experiencing it in the United States (8). A tinnitus animal model that was designed to treat utilized a high-dose of salicylate and was used to study auditory trauma associated with tinnitus. Salicylate is well known for its potent analgesic, antipyretic and anti-inflammatory activity. Administration of salicylate at specific doses can result in a unique pattern of auditory dysfunction, characterized by reversible hearing loss and tinnitus (9). Consequently, the use of animal models is frequently adopted in order to establish the condition of tinnitus in various animal species (10,11). Vascular disturbances in the cochlea have been demonstrated to result from an inhibition of cyclooxygenase (COX) by salicylate. COX participates in the arachidonic acid cascade (12,13). However, the exact mechanisms of salicylate-induced ototoxicity remain unclear. Previous studies on salicylate-induced tinnitus focused on the spontaneous activity of the auditory nerve (14). The cochlea is the major site of salicylate-induced tinnitus, since the latter can inhibit COX activity and consequently may result in synapse activation by cochlear N-methyl-D-aspartate receptors (NMDAR) via the COX pathway. Based on these results it remains controversial why high doses of aspirin can cause hearing loss, since it has been proved that inner hair cell (IHC) ribbon numbers determine the degree of auditory brain response (ABR) wave restoration (15). Despite the increase in understanding regarding the function of pre and postsynaptic regions, the molecular mechanisms underlying the alteration

Correspondence to: Dr Lin Shi or Dr Mei Lv, Department of Otorhinolaryngology, The First Affiliated Hospital of Dalian Medical University, 222 Zhongshan Road, Dalian, Liaoning 116013, P.R. China
E-mail: shilin516@sina.com
E-mail: lv_mei@163.com

[*]Contributed equally

of ribbon synapses following a lower-dose, long-duration salicylate treatment are not fully defined. A limited number of studies have focused on ribbon synapses of IHC. The majority of the laboratory studies on salicylate ototoxicity involved acute trauma models. This is due to the fact that a high-dose, short duration salicylate treatment may readily induce morphological alterations to cochlea components, which are possibly completely reversible (16-19). In addition, the majority of behavioral and neural measures of salicylate ototoxicity rely on sensitivity of the nerve as the primary indicator of impairment (9). In contrast to the altered spontaneous electrical activity in the central auditory pathway, a permanent reduction in compound action potential (CAP) amplitude was observed following chronic treatment by salicylate (20), which indicates a disorder in ribbon synapse of IHC. The present study aimed to examine whether an alteration in γ-amino butyric acid-mediated ribbon synapse inhibition may result in tinnitus and hearing loss. The specific aims of the experiment were the following: i) examination of the effect of salicylate on the hair cells and ribbon synapse of IHC and ii) examination of the association between the hearing threshold and the alteration of the ribbon synapse.

Materials and methods

Animal preparation. 2-month-old male C57BL/6J mice (18-24 g) were randomly divided into 2 groups (n=20 each). One group received saline (control group), whereas the other received salicylate (SA group; Tianjin Beilian Chemicals Co., Ltd., Tianjin, Chins). A total of 40 mice were obtained from the SPF Animal Center of Dalian Medical University (Dalian, China). The animals were housed at 20-23°C, with ~45% humidity and a 12 h light/dark circle. Animals were handled and treated according to the guidelines established by the National Institutes of Health and the Institutional Animal Care and Use Committee of the First Affiliated Hospital of Dalian Medical University and the protocol of the present study was approved by the Animal Ethical and Welfare Committee of the Dalian Medical University.

Salicylate treatments. Previous behavioral evidence of salicylate-induced tinnitus was tested at a dose of 200 mg/kg, once per day for a total period of 14 days (21). These conditions successfully established a tinnitus model in C57BL/6J mice. Sodium salicylate was dissolved in saline at a concentration of 50 mg/ml and the animals in the tinnitus group were administered salicylate solution intraperitoneally (i.p.) at a dose of 200 mg/kg, once per day, for 14 days.

Assessment of auditory function. ABR audiograms were conducted at day 14 following treatment. Mice were tested in a double blinded fashion for ABR thresholds with equipment from Intelligent Hearing Systems (Miami, FL, USA). The smart-EP v2.21 was used to generate specific acoustic stimuli and to amplify measure and display the evoked brainstem responses of mice. Mice were sedated by i.p. injection of sodium pentobarbitone (100 mg/kg; Sigma-Aldrich Merck KGaA, Darmstadt, Germany) and ABR testing was conducted in response to click stimuli. The ABR was recorded by three silver needle electrodes placed subdermally over the vertex

(positive), broadband click and tone bursts of 4, 8, 16 and 32 kHz was delivered through an insert earphone (Intelligent Hearing Systems) that was placed directly in the ear canal. Auditory thresholds which were based on the visibility and reproducibility of wave III (22) were obtained for each stimulus by variations in the sound pressure level (SPL) in 5-dB steps. The variations were conducted in a fluctuating manner to identify the lowest level at which an ABR pattern could be recognized. ABR thresholds were determined for each stimulus frequency by identifying the lowest intensity producing a reproducible ABR pattern on the computer screen (at least two consistent peaks; Fig. 1A).

Distortion Product Otoacoustic Emissions (DPOAEs) were measured using an ER-10B+ (Etymotic Research, Inc., Elk Grove Village, IL, USA) microphone coupled with two EC1 speakers. Stimuli of two primary tones f1 and f2 (f2/f1=1.2) were presented with f1=65 dB, f2=55 dB increments and swept from 8 to 32 kHz in 1/2 octave steps. Stimuli were generated and attenuated digitally (200 kHz sampling). The ear canal sound pressure was preamplified and digitized. Amplitudes of 2f1-f2 were measured based on the baseline (Fig. 1B).

Cochlear tissue processing. The mice were decapitated under deep anesthesia following treatment for 14 days. The cochleae were rapidly removed from the skull. The round and oval windows and the apex of the cochlea were dissected, and perfusion was carried out in the presence of 4% paraformaldehyde at 4°C overnight. Following fixation, the cochlea shell was decalcified with 10% EDTA for 4-6 h and subsequently separated from the basal turn under a dissecting light microscope in 0.01 mmol/l PBS solutions. The parietal gyrus of the basilar membrane was separated and the vestibular membrane and covering membranes were removed.

Immunochemistry. The separated basilar membranes were washed three times in 0.01 M PBS and preincubated for 30 min at room temperature in blocking solution of 5% normal donkey serum (S30; EMD Millipore, Billerica, MA, USA) in 0.01 M PBS. The one side of the ears corresponding to each mouse was incubated with a combination of goat anti-mouse C-terminal-binding protein 2 (CtBP2; E 16; C terminal binding protein 2, C, end of combination of protein; sc-5966; 1:200; Santa Cruz Biotechnology, Inc., Dallas, TX, USA) and rabbit anti-mouse postsynaptic dendrite 95 (PSD95; postsynaptic) antibodies (ab18258; 1:200; Abcam, Cambridge, MA, USA), whereas the other side was incubated with a combination of goat anti-mouse CtBP2 and rabbit anti-mouse GluR2/3 antibodies (AB1506; 1:100; EMD Millipore) at 4°C overnight. The incubated samples were washed in 0.01 M PBS three times and incubated in donkey anti-goat 488 (ab150129; 1:200; Abcam) and donkey anti-rabbit 568 antibodies (ab150129; 1:200; Abcam) at room temperature for 60 min. The samples were subsequently, washed three times. A limited volume (~40 µl) of DAPI (sc-3598; Santa Cruz Biotechnology, Inc.) was added dropwise in the slide and the basement membranes were tiled under a dissecting microscope with the coverslip covering the slide. The samples were viewed directly with fluorescent microscopy to test the specificity of the primary antibody, as detailed below.
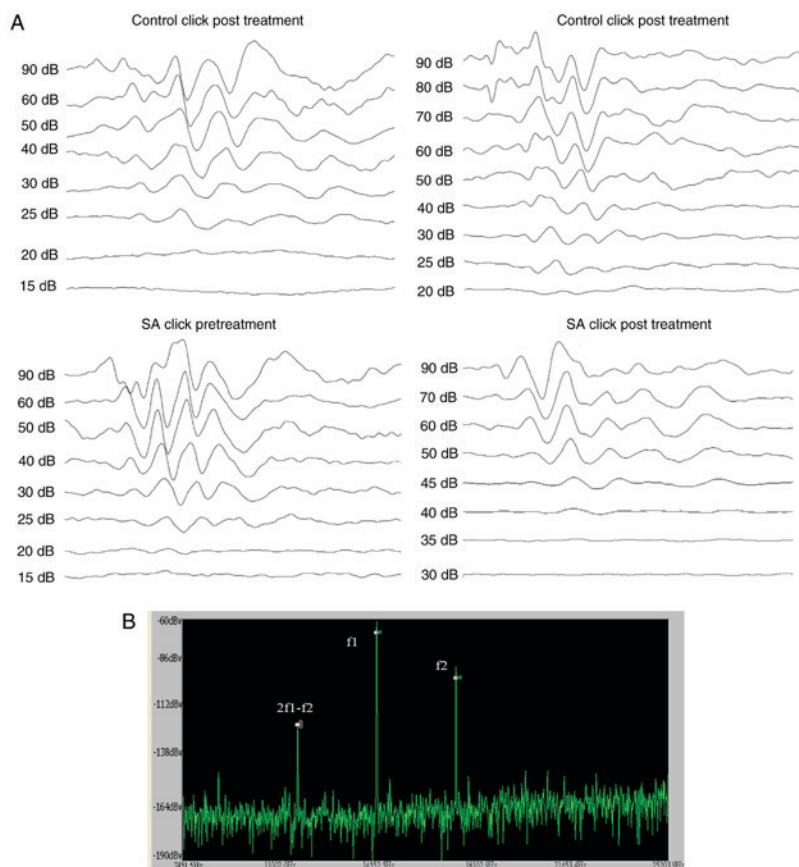
Figure 1. ABR audiograms and DPOAE of the two groups of mice prior to and following treatment. (A) Waveforms of ABR evoked by clicks of the two groups. (B) Illustrations of the methods to measure DPOAE. When DPOAE was measured, f1 and f2 were connected to the earpiece. The f2 was set at 4, 8, 16 and 32 kHz. The f2/f1 ratio was set at 1.2. The intensity of f2=55 dB, f1=65 dB. Amplitudes of 2f1-f2 were measured. APR, auditory brainstem response; DPOAE, distortion product otoacoustic emission; SA, salicylate.

Laser scanning confocal microscopy imaging. The laser scanning confocal microscope was an Olympus FV1000 configuration (Olympus Corporation, Tokyo, Japan) with 180X oil immersion objective. The excitation wavelengths were 488 and 568 nm for the two antibodies, respectively. Sequence scanning was conducted in cochlear IHCs with an interval of 0.12 μm. Due to immunohistochemical double-staining that was carried out at 488 and 568 nm as the emission wavelengths of the secondary antibodies, the double-labeled fluorescence appeared orange in color. The sequence scanning initiated in the region of the color pair fluorescence, whereas it was stopped in the region where the fluorescein color pairs disappeared. The scanning interval for sequential scanning was set to 0.15 μm in order to ensure that each synapse would be marked to the size of mature IHC ribbon synapses that ranged from 150 to 200 nm (23). Following completion of serial scanning, the two-dimensional image files were opened successively using Autodesk 3Ds Max software (2010 release; Autodesk, Inc., San Rafael, CA, USA). The fluorescein color pairs were marked by spheres in the first two-dimensional image and the process was repeated for subsequent images. Finally, the number of spheres was counted and the synapses were reconstructed in 3D images. The sequence scanning for the parietal gyrus of 60 basilar membranes was carried out. A total of one visual field was selected from each basilar membrane for scanning and 60 files were obtained.

Marking of IHC ribbon synapses and counting the number of ribbon synapses. Serial scanning generated two-dimensional images, which were used to mark IHC ribbon synapses. The image files were opened successively from top to bottom using 3Ds Max Software. The images were magnified in a 'zoomed top view' to identify IHC ribbon synapses. The orange fluorescence that indicated the IHC ribbon synapses appeared in each image and was initially marked by a sphere. The size of the sphere was adjusted to match the size of the area of the orange fluorescence. Prior to the analysis of the orange fluorescence of each image, the previous marked image was opened for comparison. Fluorescence analysis was omitted to avoid repetitive labeling of the same synapse provided the orange fluorescence appeared at the same location of the previous image. All the images were overlapped and the number of spheres (indicating IHC ribbon synapses) was counted using the layer manager of 3Ds Max.

Statistical analysis. The ABR was repeated 3 times, and an average was calculated as the threshold of the mouse. Immunohistochemistry was performed in every mouse with both ears. Statistical analyses were carried out using SPSS 15.0 software (SPSS, Inc., Chicago, IL, USA). All data are expressed as the mean ± standard error of the mean. The control and salicylate-treated ABR audiograms (specifically the SPLs) of the groups were compared, using a one-way analysis of variance. For multiple comparisons of the number
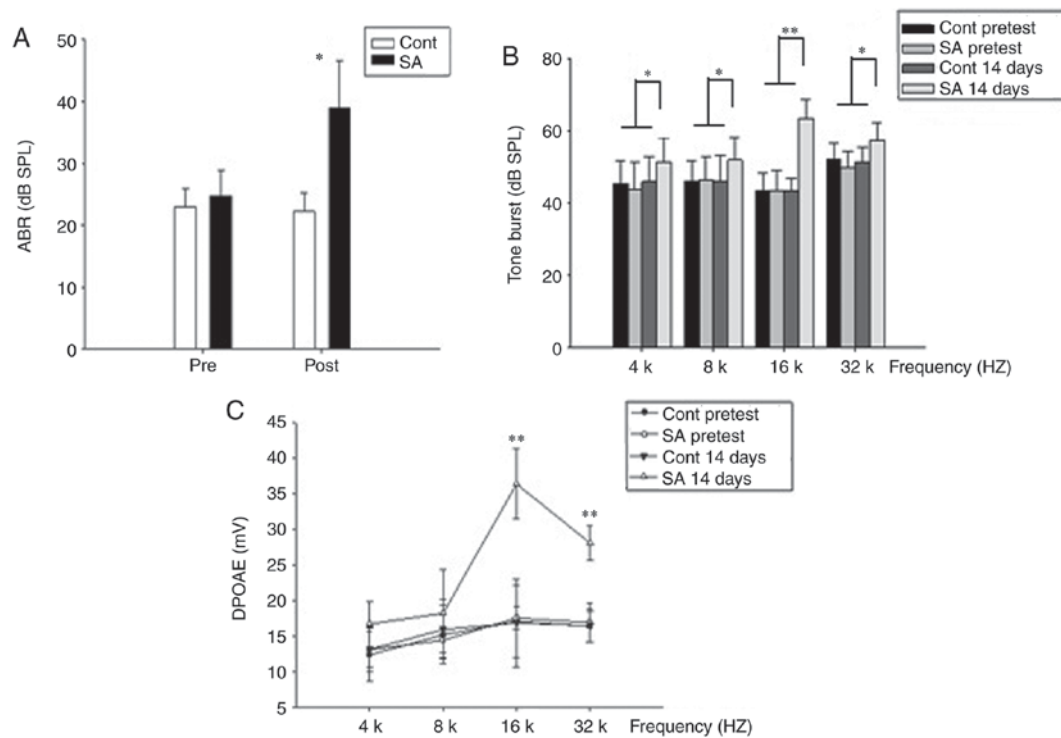
Figure 2. The hearing threshold is elevated following intraperitoneal injection of sodium salicylate (SA group) compared with injection of saline (control group). (A) In the control group, the mean ABR threshold of mice pretreatment was 23.0±2.99 dB SPL (n=20) and 22.25±3.02 dB SPL post treatment (n=20), respectively. The mean ABR threshold of SA group mice pretreatment was 24.75±4.13 dB SPL (n=20) and 39.0±7.54 dB SPL post treatment (n=20), respectively. ABR thresholds of the SA group were compared to the control group. The results were presented as the mean ± standard error of the mean of SPL (dB). *P<0.05; post-SA group vs. the control group. (B) On the 14th post-treatment day, thresholds elevation demonstrated a significant improvement at 16 and 32 kHz in SA group compared with those in the control group. *P<0.05 and **P<0.01. Thresholds at 4 and 8 kHz are slightly higher in SA group compared with those in the control group. (C) In the control group, DPOAEs in 4, 8, 16, 32 kHz were 13.17±3.12, 15.95±4.17, 16.89±6.16, 16.5±2.34 at 14th day post treatment. A dramatic increase of the DPOAE amplitude at 14th day in SA group in 16, 32 kHz was presented, 36.44±4.93, 28.14±2.38, respectively. **P<0.01 vs. the control group. APR, auditory brainstem response; SPL, sound pressure level; SA, salicylate; Cont, control; DPOAE, distortion product otoacoustic emission.

of IHC ribbon synapses, Tukey's post-hoc multiple comparison test was used. Multivariate regression analysis was used to analyze the associations of mismatched synapses and hearing loss. P<0.05 was considered to indicate a statistically significant difference.

Results

Elevated of the hearing threshold following i.p. injection of sodium salicylate (tinnitus group) but not following injection of saline (control group). Using click stimuli that were spectrally dominated by frequencies <32 kHz, ABR thresholds of the tinnitus and control groups were detected prior to the salicylate/sodium treatment and at the 14th day post-treatment. The ABR thresholds for the pre and post treatment groups were 24.75±4.13 and 39.0±7.54, respectively for the tinnitus group, and 23.0±2.99 and 22.25±3.02, for the control group (Fig. 2A), suggesting mild hearing loss in the tinnitus group. Furthermore, the hearing loss was significantly different in the tinnitus group compared with the control group on the 14th day post-treatment (P<0.05). Additionally, the salicylate treatment caused a significant ABR threshold elevation across all frequencies especially the high frequencies (P<0.05). On the 14th day post-treatment, statistically significant threshold alterations were demonstrated at 16 and 32 kHz (Fig. 2B; P<0.01) in the salicylate group, indicating increasing hearing impairment.

Contrary to the ABR, an increase in amplitude of DPOAE was obtained following salicylate treatment. At 16 kHz, the DPOAE amplitude increased most significantly (Fig. 2C; P<0.01).

Irritation from salicylate does not affect the characteristics of cochlear hair cells. In the mammalian cochlea, IHC are responsible for voice encoding, whereas the outer hair cells are responsible for sound amplification (24). In the present study, DAPI nuclear staining was used to investigate whether salicylate exposure could induce morphological alterations to cochlear hair cells. OHCs and IHCs exhibited normal morphology as indicated by the nuclei of the hair cells throughout the period of salicylate exposure (Fig. 3A; DAPI nuclei staining where indicated). This result suggested that cochlear hair cells are not affected by salicylate exposure. Furthermore, the DPOAEs of salicylate group indicated normal function of OHCs following 14-day salicylate treatment (Fig. 2C).

Salicylate induces number alterations of IHC ribbon synapses. IHC ribbon synapses are excitable synapses that encode sound signals. In the present study, since the DPOAEs of the salicylate group increased in high frequencies, the basic gyri of basic membranes between the two groups were compared (Fig. 3B). The specific presynaptic protein RIBEYE/CtBP2 was labeled with an anti-CtBP2 antibody that is located solely in ribbon synapses (25,26). The right or left ear was randomly selected
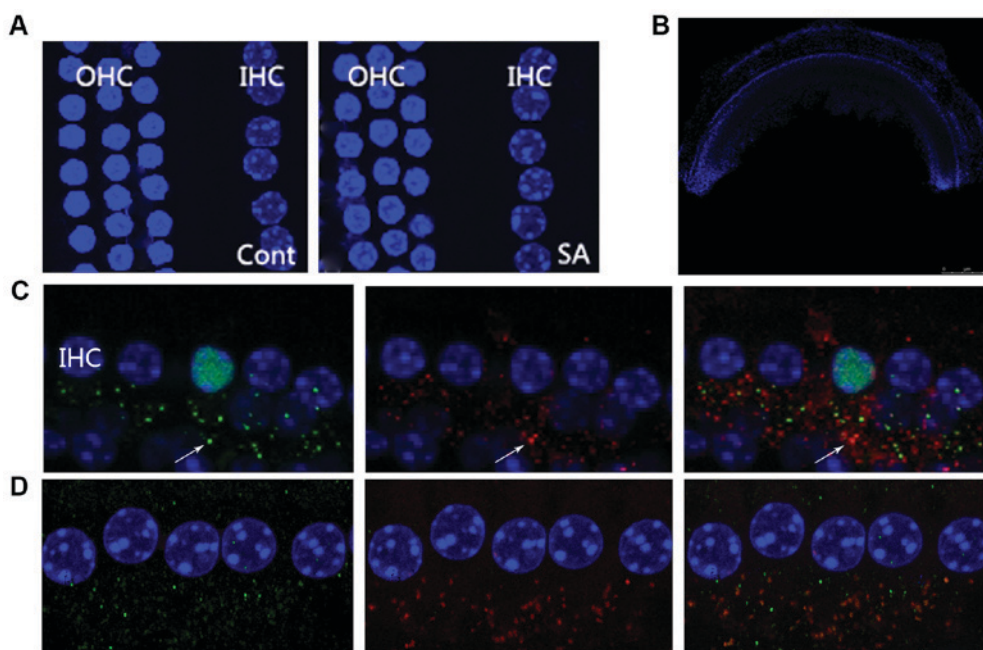
Figure 3. Irritation from salicylate does not affect the morphology of cochlear hair cells, although it increases the number of IHCs at the ribbon synapse. (A) Microscopy images reveal a normal morphological array in the control and SA groups. A row of IHCs and three rows of OHCs were included. Blue labeling indicates DAPI-positive hair cell nuclei. Scale bar=50 μm. (B) The morphology of the basical turn of basilar membrane. Scale bar=500 μm. (C) CtBP2 of the control group, the presynaptic marker of IHC ribbon synapses, were labeled by anti-CtBP2 antibody in green beneath the IHCs as indicated by the white arrow. Postsynaptic receptors were labeled by a PSD95 antibody in red beneath the IHCs as indicated by the white arrow. The merged image indicates an intact ribbon synapse in orange fluorescence beneath the IHCs depicted by the white arrow. Scale bar=10 μm. (D) CtBP2 of the SA group at the 14th day following salicylate treatment, including CtBP2 and PSD95, were observed in increasing numbers. IHCs, inner hair cells; OHCs, outer hair cells; PSD95, postsynaptic density protein 95; CtBP2, c-terminal binding protein 2; SA, salicylate; Cont, control.

and identified using an PSD95 antibody which binds to post-synaptic dendrites (15,27), whereas the other side of the ears was identified using an anti-GluR2/3 antibody, which binds to α-amino-3-hydroxy-5-methyl-4-isoxa-zole-propionate receptors (AMPARs) (28,29). A merged image that included labeling of the RIBEYE/CtBP2 protein and NMDARs and/or AMPARs indicated an intact synapse (Fig. 3B and C).

The 3Ds Max Software package can effectively reconstruct a template model of anatomical targets using two-dimensional images (30-34). The authors' previous study demonstrated that 3Ds Max can be used to calculate the number of IHC ribbon synapses in healthy C57 mice. Therefore, 3Ds Max is considered appropriate for quantitative analysis of IHC ribbon synapses when mice are stimulated with salicylate treatment. Using this method, it was noted that the number of RIBEYE/CtBP2 and PSD95 was increased to a similar level (Fig. 4A). The merged image that included labeling of the RIBEYE/CtBP2 and PSD95 proteins was 17.15±1.39 and 16.7±1.69, respectively in the control and tinnitus groups prior to treatment and 16.4±1.73 and 21.4±1.70 at the 14th day of treatment, respectively. However, the decrease of AMPARs was detected in the tinnitus group (Fig. 4B). The fluorescence value of GluR2/3 was 16.40±1.73 and 16.7±1.69 in the control and tinnitus groups prior to treatment, and 16.30±1.53 and 3.9±3.95 at the 14th day of treatment, respectively. Mismatch of CtBP2 and GluR2/3 was associated with hearing loss following salicylate treatment (Fig. 4C and D).

The alteration in the number of ribbon synapses suggested that IHC ribbon synapses were significantly affected by exposure to salicylate. Therefore, IHC ribbon synapses were demonstrated to be susceptible to salicylate exposure. Significant deterioration of the hearing thresholds can be caused by severe ribbon loss, despite intact OHC functions (35). This result demonstrated that tinnitus animals with increased NMDAR and transmitter release of the tinnitus animals that exhibited higher ABR thresholds.

Discussion

The results of the present study demonstrate that salicylate improved DPOAE amplitudes during treatment. These results are consistent with the view that salicylate enhances OHC function by upregulating prestin expression, which increases OHC electromotility (20). Although DPOAEs were enhanced, a reduction in ABR amplitude was observed unexpectedly. Thresholds recorded 14 days following drug treatments demonstrated a decrease compared with the control. These results, which were unexpected, demonstrated that long term treatment with salicylate may result in auditory function impairment, but the target organ was not OHC.

The present study was designed to examine the mechanisms that are associated with hearing loss and alteration of ribbon synapses, following induction of tinnitus by salicylate in mice. The difficulties associated with measuring the activity of NMDARs at adult synapses, have produced conflicting results about their expression levels (36). Several studies reported no detectable current on spiral ganglion somata and/or calcium alteration in postsynaptic afferent boutons induced by NMDA application. Cochlear synaptic transmission was carried out by AMPAR in the absence of NMDARs (34-36). In contrast
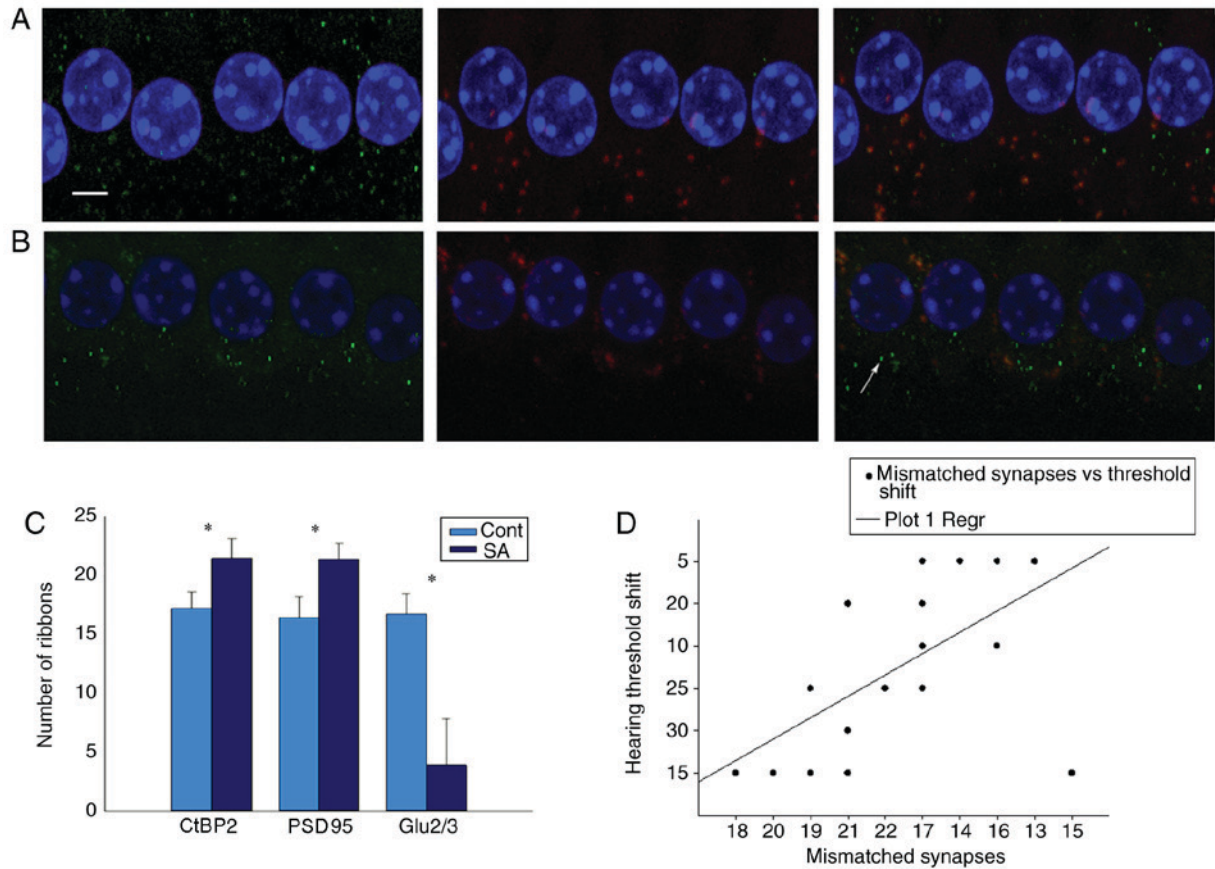
Figure 4. Salicylate reduces the number of post synaptic AMPARs, which causes mismatch between pre and post synapses. (A) CtBP2 of the control group, the presynaptic marker of IHC ribbon synapses, is labeled by an anti-CtBP2 antibody in green beneath the IHCs. Postsynaptic receptors are labeled by a GluR2/3 antibody in red beneath the IHCs. Merged image indicates an intact ribbon synapse in orange fluorescence beneath the IHCs. Scale bar=10 μm. (B) CtBP2 of the SA group at the 14th day following salicylate treatment, the presynaptic marker of IHC ribbon synapses (CtBP2) increased, while the postsynaptic marker (GluR2/3) decreased. Solitary green marks indicate a mismatched synapse beneath the IHCs indicated by white arrow. (C) Numbers of pre- and post-synaptic receptors of the SA group were compared to the control group at the 14th day following treatment. Results are presented as the mean ± standard error of the mean of SPL (dB). The merged image labeling RIBEYE/CtBP2 and PSD95 was 16.4±1.73 and 21.4±1.70 in the control group and tinnitus group at the 14th day following treatment. However, decrease of AMPARs was detected in tinnitus group. The number of GluR2/3 was 16.40±1.73, 3.9±3.95, at the 14th day following treatment, respectively; *P<0.05 vs. the control. (D) There was a significant correlation between the number of mismatched synapses and the hearing threshold (r=-0.904, P<0.01). PSD95, postsynaptic density protein 95; CtBP2, c-terminal binding protein 2; AMPARs, α-amino-3-hydroxy-5-methyl-4-isoxazole-propionate receptors; IHC, inner hair cells; Cont, control; SA, salicylate.

to the aforementioned studies, the induction of tinnitus by COX blockers (salicylate and mefenamate) was mediated by cochlear NMDARs. In the present study, the data indicated a discrepancy between PSD95 and Glu2/3 that suggested the presence of NR1 and NR2B at the postsynaptic density of the IHC synapses. The results of the present study, directly suggest that NMDARs exist at this ribbon synapse. This is inconsistent with a previous study that reported the presence of NMDARs at the IHC synapses by Patch-clamp recordings (37). Consequently, it was hypothesized that salicylate may modulate the IHC synaptic neurotransmission via NMDARs at the IHC synapses. To the best of our knowledge the results of the present study are considered novel.

Salicylate increased the levels of arachidonic acid in the entire part of the cochlea *in vivo* by enabling the activation of NMDARs (38). Therefore, whether the altered number of IHC ribbon synapses is responsible for hearing loss remains undiscovered. The data reported in the current study indicated that other cochlear components, including OHCs and IHCs, were not markedly affected. This supports the idea that OHCs and IHCs may not be responsible for the impaired hearing

induced by exposure to a low dose of salicylate. Therefore, it is reasonable to consider that IHC ribbon synapses may be responsible for the induction of tinnitus and impaired hearing observed in this study. Salicylate caused an excitatory effect in the presence of GYKI 53784 that resulted in complete inhibition of AMPAR (39). This result contradicts the hypothesis that the activation of IHC NMDA auto receptors as a unique mechanism of salicylate action. The result that an mGluR2/3 agonist significantly reverses the expression of the dysfunctional NMDAR in the MK-801 model of schizophrenia indicates a direct competitive inhibition (39). These findings were consistent with the data presented in the present study. Furthermore, it was demonstrated that the number of IHC ribbon synapses increased on the 14th day following salicylate exposure, whereas CtBP2 increased in a synchronous manner with PSD95. However, a dramatic reduction in the number of Glu2/3 occurred at the 14th day.

Researchers demonstrated that salicylate increased auditory nerve fiber spontaneous activity. During perilymphatic perfusion of salicylate an increase in the spontaneous spiking rate was noted that may occur in part due to an activation of the NMDA

auto receptors on the IHCs. This process would in turn increase glutamate release in the central nervous system, as described in previous studies (40-43). In addition, the overall responsiveness of a fiber of the spiral ganglion neuron (SGN) may be regulated postsynaptically. This mechanism has previously been demonstrated to exist in the postsynaptic boutons of SGN (44) indicating that the activation of the NMDAR by salicylate increases the glutamate receptor activity in the IHC synaptic region. This may provide an explanation of the protective effect of salicylate on mice against hearing loss caused by gentamicin ototoxicity (45). However, the present study is consistent with other studies that demonstrated a hearing loss following salicylate treatment. The data suggest that the hearing loss is due to the mismatch between the presynapses and postsynapses of the AMPR. The mismatch between pre and post synapses would be expected to be functionally destructive, due to the lack of synaptic transmission of the pre-synaptic ribbons (46).

Since inhibitory synapse has been demonstrated before (47,48), a great deal was known about the molecular control of excitatory synapse formation. It was speculated that functional circuits depend on the proper balance of synaptic excitation and inhibition to process sensory information and to perform motor and cognitive tasks. Excitatory-inhibitory imbalances and synaptic dysfunction lead to neurological and psychiatric disorders (47,48). The latest discovery of Zugaib *et al* (49) demonstrated endocannabinoid-dependent depolarization-induced suppression of excitation in glycinergic neurons were enhanced as mice were exposed to prolonged high doses of salicylate. The results pointed to an increased inhibition of the dorsal cochlear nucleus (DCN) inhibitory cartwheel neuron during depolarizations, which is potentially significant for DCN hyperactivity and tinnitus generation. Therefore, whether the enhanced NMDARs in the present study were inhibitory synapses as demonstrated with DCN remains unclear. Further molecular tests are required to verify it.

The current study demonstrates the previously mentioned hypothesis and offers a comprehensive analysis regarding the explanation of the exact etiology of the hearing loss. The alteration in the number of AMPR as opposed to the number of ribbons appears to be the primary reason for hearing loss.

In conclusion, the present study suggests that a different degree of damage of the first synapse occurs within the auditory pathway and the IHC synapse. The data revealed that exposure to a low-dose of salicylate over a long-duration could induce quantitative alterations in the number of the pre and postsynaptic ribbons of IHCs, while it did not affect the number of the cochlear hair cells. IHC ribbon synapses were the primary targets of salicylate and may be responsible for tinnitus and hearing loss. The current study provides direct evidence of a novel pharmacological profile of salicylate that induces an increase in arachidonic acid levels. This increase enabled the activation of NMDAR at the IHC ribbons. The present study hypothesized that the increase in the ribbon synapses that is caused by excessive activation of NMDAR may induce abnormal spontaneous activity of auditory nerve fibers, which could lead to the induction of tinnitus. The present study further indicated a competitive inhibition between NMDAR and AMPAR that induced a mismatch between ribbons and AMPAR that in turn caused hearing loss. Although, the mechanism of the modulation of the NMDA/AMPAR ratio in IHC cells remains unknown, the present study provides a novel molecular mechanism that accounts for the formation of tinnitus at the periphery of the auditory system.

Acknowledgements

Not applicable.

Funding

Availability of data and materials

The datasets used and/or analyzed during the current study are available from the corresponding author on reasonable request.

Author's contributions

LS was responsible for the conception and design of the study. ML conducted and supervised the experiments. WC and HW conducted the experiments and wrote the main manuscript text. YC and XM prepared all the figures. YL performed statistical analysis. XR collected the data. All authors reviewed the manuscript.

Ethics approval and consent to participate

The present study is supported by the Education Foundation of Liaoning province and the protocol was approved by the Animal Ethical and Welfare Committee of the Dalian Medical University (Dalian, China).

Patient consent for publication

Not applicable.

Competing interests

The authors declare that they have no competing interests.

References

1. Fresca TM, Salvi RF and Archela RS: Dimensões do espaço paranaense. Editora UEL, Londrina, 2002.
2. Moller AR: Pathophysiology of tinnitus. Otolaryngol Clin North Am 36: 249-266, v-vi, 2003.
3. Jastreboff PJ: Tinnitus retraining therapy. Prog Brain Res 166: 415-423, 2007.
4. Zenner HP, Pfister M and Birbaumer N: Tinnitus sensitization: Sensory and psychophysiological aspects of a new pathway of acquired centralization of chronic tinnitus. Otol Neurotol 27: 1054-1063, 2006.
5. Puel JL and Guitton MJ: Salicylate-induced tinnitus: molecular mechanisms and modulation by anxiety. Prog Brain Res 166: 141-146, 2007.
6. Leaver AM, Renier L, Chevillet MA, Morgan S, Kim HJ and Rauschecker JP: Dysregulation of limbic and auditory networks in tinnitus. Neuron 69: 33-43, 2011.
7. Langguth B, Salvi R and Elgoyhen AB: Emerging pharmacotherapy of tinnitus. Expert Opin Emerg Drugs 14: 687-702, 2009.

8. Shargorodsky J, Curhan GC and Farwell WR: Prevalence and characteristics of tinnitus among US adults. Am J Med 123: 711-718, 2010.

9. Cazals Y: Auditory sensori-neural alterations induced by salicylate. Prog Neurobiol 62: 583-631, 2000.

10. Jastreboff PJ, Brennan JF, Coleman JK and Sasaki CT: Phantom auditory sensation in rats: An animal model for tinnitus. Behav Neurosci 102: 811-822, 1988.

11. Jastreboff PJ, Brennan JF and Sasaki CT: An animal model for tinnitus. Laryngoscope 98: 280-286, 1988.

12. Escoubet B, Amsallem P, Ferrary E and Tran Ba Huy P: Prostaglandin synthesis by the cochlea of the guinea pig. Influence of aspirin, gentamicin and acoustic stimulation. Prostaglandins 29: 589-599, 1985.

13. Jung TT, Miller SK, Rozehnal S, Woo HY, Park YM and Baer W: Effect of round window membrane application of salicylate and indomethacin on hearing and levels of arachidonic acid metabolites in perilymph. Acta Otolaryngol Suppl 493: 81-87, 1992.

14. Martin WH, Schwegler JW, Scheibelhoffer J and Ronis ML: Salicylate-induced changes in cat auditory nerve activity. Laryngoscope 103: 600-604, 1993.

15. Singer W, Zuccotti A, Jaumann M, Lee SC, Panford-Walsh R, Xiong H, Zimmermann U, Franz C, Geisler HS, Köpschall I, *et al*: Noise-induced inner hair cell ribbon loss disturbs central arc mobilization: A novel molecular paradigm for understanding tinnitus. Mol Neurobiol 47: 261-279, 2013.

16. Bernstein JM and Weiss AD: Further observations on salicylate ototoxicity. J Laryngol Otol 81: 915-925, 1967.

17. Didier A, Miller JM and Nuttall AL: The vascular component of sodium salicylate ototoxicity in the guinea pig. Hear Res 69: 199-206, 1993.

18. McFadden D, Plattsmier HS and Pasanen EG: Aspirin-induced hearing loss as a model of sensorineural hearing loss. Hear Res 16: 251-260, 1984.

19. McFadden D, Plattsmier HS and Pasanen EG: Temporary hearing loss induced by combinations of intense sounds and nonsteroidal anti-inflammatory drugs. Am J Otolaryngol 5: 235-241, 1984.

20. Chen GD, Kermany MH, D'Elia A, Ralli M, Tanaka C, Bielefeld EC, Ding D, Henderson D and Salvi R: Too much of a good thing: Long-term treatment with salicylate strengthens outer hair cell function but impairs auditory neural activity. Hear Res 265: 63-69, 2010.

21. Yu N, Zhu ML, Johnson B, Liu YP, Jones RO and Zhao HB: Prestin up-regulation in chronic salicylate (aspirin) administration: An implication of functional dependence of prestin expression. Cell Mol Life Sci 65: 2407-2418, 2008.

22. Bourre JM, Durand G, Erre JP and Aran JM: Changes in auditory brainstem responses in alpha-linolenic acid deficiency as a function of age in rats. Audiology 38: 13-18, 1999.

23. Moser T, Neef A and Khimich D: Mechanisms underlying the temporal precision of sound coding at the inner hair cell ribbon synapse. J Physiol 576: 55-62, 2006.

24. Starr A, Picton TW, Sininger Y, Hood LJ and Berlin CI: Auditory neuropathy. Brain 119: 741-753, 1996.

25. Sudhof TC: The synaptic vesicle cycle. Annu Rev Neurosci 27: 509-547, 2004.

26. Roux I, Safieddine S, Nouvian R, Grati M, Simmler MC, Bahloul A, Perfettini I, Le Gall M, Rostaing P, Hamard G, *et al*: Otoferlin, defective in a human deafness form, is essential for exocytosis at the auditory ribbon synapse. Cell 127: 277-289, 2006.

27. Maier W, Bednorz M, Meister S, Roebroek A, Weggen S, Schmitt U and Pietrzik CU: LRP1 is critical for the surface distribution and internalization of the NR2B NMDA receptor subtype. Mol Neurodegener 8: 25, 2013.

28. Wang Q and Green SH: Functional role of neurotrophin-3 in synapse regeneration by spiral ganglion neurons on inner hair cells after excitotoxic trauma in vitro. J Neurosci 31: 7938-7949, 2011.

29. Biou V, Bhattacharyya S and Malenka RC: Endocytosis and recycling of AMPA receptors lacking GluR2/3. Proc Natl Acad Sci USA 105: 1038-1043, 2008.

30. Ma B, Wang L, von Wasielewski R, Lindenmaier W and Dittmar KE: Serial sectioning and three-dimensional reconstruction of mouse Peyer's patch. Micron 39: 967-975, 2008.

31. Filippi S, Motyl B and Bandera C: Analysis of existing methods for 3D modelling of femurs starting from two orthogonal images and development of a script for a commercial software package. Comput Methods Programs Biomed 89: 76-82, 2008.

32. Gruska M, Medalia O, Baumeister W and Leis A: Electron tomography of vitreous sections from cultured mammalian cells. J Struct Biol 161: 384-392, 2008.

33. Punge A, Rizzoli SO, Jahn R, Wildanger JD, Meyer L, Schönle A, Kastrup L and Hell SW: 3D reconstruction of high-resolution STED microscope images. Microsc Res Tech 71: 644-650, 2008.

34. Nakagawa T, Komune S, Uemura T and Akaike N: Excitatory amino acid response in isolated spiral ganglion cells of guinea pig cochlea. J Neurophysiol 65: 715-723, 1991.

35. Ruel J, Chen C, Pujol R, Bobbin RP and Puel JL: AMPA-preferring glutamate receptors in cochlear physiology of adult guinea-pig. J Physiol 518: 667-680, 1999.

36. Glowatzki E and Fuchs PA: Transmitter release at the hair cell ribbon synapse. Nat Neurosci 5: 147-154, 2002.

37. Ruel J, Chabbert C, Nouvian R, Bendris R, Eybalin M, Leger CL, Bourien J, Mersel M and Puel JL: Salicylate enables cochlear arachidonic-acid-sensitive NMDA receptor responses. J Neurosci 28: 7313-7323, 2008.

38. Khimich D, Nouvian R, Pujol R, Tom Dieck S, Egner A, Gundelfinger ED and Moser T: Hair cell synaptic ribbons are essential for synchronous auditory signalling. Nature 434: 889-894, 2005.

39. Xi D, Li YC, Snyder MA, Gao RY, Adelman AE, Zhang W, Shumsky JS and Gao WJ: Group II metabotropic glutamate receptor agonist ameliorates MK801-induced dysfunction of NMDA receptors via the Akt/GSK-3β pathway in adult rat prefrontal cortex. Neuropsychopharmacology 36: 1260-1274, 2011.

40. Berretta N and Jones RS: Tonic facilitation of glutamate release by presynaptic N-methyl-D-aspartate autoreceptors in the entorhinal cortex. Neuroscience 75: 339-344, 1996.

41. Breukel AI, Besselsen E, Lopes da Silva FH and Ghijsen WE: A presynaptic N-methyl-D-aspartate autoreceptor in rat hippocampus modulating amino acid release from a cytoplasmic pool. Eur J Neurosci 10: 106-114, 1998.

42. Woodhall G, Evans DI, Cunningham MO and Jones RS: NR2B-containing NMDA autoreceptors at synapses on entorhinal cortical neurons. J Neurophysiol 86: 1644-1651, 2001.

43. Luccini E, Musante V, Neri E, Raiteri M and Pittaluga A: N-methyl-D-aspartate autoreceptors respond to low and high agonist concentrations by facilitating, respectively, exocytosis and carrier-mediated release of glutamate in rat hippocampus. J Neurosci Res 85: 3657-3665, 2007.

44. Chen Z, Kujawa SG and Sewell WF: Auditory sensitivity regulation via rapid changes in expression of surface AMPA receptors. Nat Neurosci 10: 1238-1240, 2007.

45. Mazurek B, Lou X, Olze H, Haupt H and Szczepek AJ: In vitro protection of auditory hair cells by salicylate from the gentamicin-induced but not neomycin-induced cell loss. Neurosci Lett 506: 107-110, 2012.

46. Shi L, Liu L, He T, Guo X, Yu Z, Yin S and Wang J: Ribbon synapse plasticity in the cochleae of Guinea pigs after noise-induced silent damage. PLoS One 8: e81566, 2013.

47. Chubykin AA, Atasoy D, Etherton MR, Brose N, Kavalali ET, Gibson JR and Südhof TC: Activity-dependent validation of excitatory versus inhibitory synapses by neuroligin-1 versus neuroligin-2. Neuron 54: 919-931, 2007.

48. Mishra A, Traut MH, Becker L, Klopstock T, Stein V and Klein R: Genetic evidence for the adhesion protein IgSF9/Dasm1 to regulate inhibitory synapse development independent of its intracellular domain. J Neurosci 34: 4187-4199, 2014.

49. Zugaib J and Leao RM: Enhancement of endocannabinoid-dependent depolarization-induced suppression of excitation in glycinergic neurons by prolonged exposure to high doses of salicylate. Neuroscience 376: 72-79, 2018.